

7. H. Z. Massoud, Ph.D. Thesis, Stanford University, Stanford, CA (1983).
8. H. Z. Massoud, J. D. Plummer, and E. A. Irene, *This Journal*, **132**, 2685 (1985).
9. H. Z. Massoud, J. D. Plummer, and E. A. Irene, *ibid.*, **132**, 1745 (1985).
10. E. A. Irene, H. Z. Massoud, and E. Tierney, *ibid.*, **133**, 1253 (1986).
11. E. A. Lewis, E. Kobeda, and E. A. Irene, in "Semiconductor Silicon 1986," H. R. Huff, T. Abe, and B. Kolbesen, Editors, p. 416, The Electrochemical Society Softbound Proceedings, Series, Pennington, NJ (1986).
12. W. A. Pliskin and G. P. Gnall, *This Journal*, **111**, 872 (1964).
13. F. Rochet, B. Agius, and S. Rigo, *ibid.*, **131**, 914 (1984).
14. U. R. Evans, "The Corrosion and Oxidation of Metals," pp. 819-859, Edward Arnold and Company, London (1960).
15. B. E. Deal and A. S. Grove, *J. Appl. Phys.*, **36**, 3770 (1965).
16. R. Ghez and Y. J. van der Meulen, *This Journal*, **119**, 1100 (1972).
17. N. F. Mott, *Proc. R. Soc. London, Ser. A*, **376**, 207 (1981).
18. P. O. Hahn and M. Henzler, *J. Vac. Sci. Technol. A*, **2**, 574 (1984).
19. W. A. Tiller, *This Journal*, **127**, 619 (1980).
20. W. A. Tiller, *ibid.*, **127**, 625 (1980).
21. E. A. Irene, *J. Appl. Phys.*, **54**, 5416 (1983).
22. E. P. EerNisse, *Appl. Phys. Lett.*, **35**, 8 (1979).
23. E. A. Irene, D. W. Dong, and R. J. Zeto, *This Journal*, **127**, 396 (1980).
24. E. Kobeda and E. A. Irene, *J. Vac. Sci. Technol.*, **B**, **4**, 720 (1986).
25. E. Kobeda and E. A. Irene, *ibid.*, **5**, 15 (1987).
26. R. H. Doremus, *This Solid Films*, **122**, 191 (1984).
27. A. Fargeix and G. Ghibado, *J. Appl. Phys.*, **54**, 153 (1983).
28. A. Fargeix and G. Ghibado, *ibid.*, **56**, 589 (1984).
29. R. B. Marcus and T. T. Sheng, *ibid.*, **129**, 1278 (1982).
30. J. K. Srivastava and E. A. Irene, *ibid.*, **132**, 2815 (1985).
31. C. K. Huang, R. J. Jaccodine, and S. R. Butler, Abstract 394, p. 595, The Electrochemical Society Extended Abstracts, Vol. 86-2, San Diego, CA, Oct. 19-24, 1986.
32. E. P. EerNisse, *Appl. Phys. Lett.*, **30**, 290 (1977).
33. W. Kern and D. A. Puotinen, *RCA Rev.*, **31**, 187 (1970).
34. F. N. Schwettman, K. L. Chiang, and W. A. Brown, Abstract 276, p. 688, The Electrochemical Society Extended Abstracts, Vol 78-1, Seattle, WA, May 21-26, 1978.
35. G. Gould and E. A. Irene, *This Journal*, **134**, 1031 (1987).
36. Y. J. van der Meulen and N. C. Hien, *J. Opt. Soc. Am.*, **64**, 804 (1974).
37. S. I. Raider, R. A. Gdula, and J. R. Petrak, *Appl. Phys. Lett.*, **27**, 150 (1975).
38. E. A. Irene, *Philos. Mag.*, **B**, **55**, 131 (1987).
39. K. Ueda and M. Inoue, *Surf. Sci.*, **161**, L578 (1985).
40. B. Z. Olshansky and A. A. Shklyayev, *ibid.*, **82**, 445 (1979).

The Effects of Chemical Oxide on the Deposition of Tungsten by the Silicon Reduction of Tungsten Hexafluoride

M. Wong,* N. Kobayashi,¹ R. Browning, D. Paine,² and K. C. Saraswat**

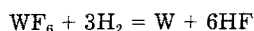
Center for Integrated Systems, Stanford University, Stanford, California 94305

ABSTRACT

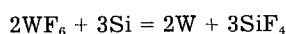
The effects of thin (chemical) oxide grown during the chemical cleaning of silicon wafers on the silicon reduction of tungsten hexafluoride have been investigated. Unlike tungsten deposition on samples without the chemical oxide, deposition thickness on those with the chemical oxide was found to be unlimited. Inspection by cross-sectional SEM and TEM revealed the existence of microchannels penetrating the tungsten film, reaching all the way from the surface of the film to the tungsten/silicon interface. These channels enable tungsten hexafluoride to reach the substrate, thus causing unlimited tungsten growth.

The low pressure chemical vapor deposition (LPCVD) of tungsten is of interest for many VLSI applications. Selective deposition finds applications for contact diffusion barriers (1, 2), resistance shunts for polysilicon gates (3), and via filling for planarization (4). Nonselective deposition finds applications for gate level interconnects (5) and via filling by etchback (6).

One of the most commonly used vapor deposition methods for tungsten is the hydrogen reduction of tungsten hexafluoride (7, 8)



Using cross-sectional TEM, Stacy *et al.* (9) observed a thin interfacial layer, possibly an oxide, separating the tungsten film into two layers. They concluded that hydrogen reduction was responsible for forming the upper tungsten layer, while the lower layer resulted from recessed tungsten growth via the silicon reduction of tungsten hexafluoride



Thus, even with hydrogen present in the deposition ambient, the silicon reduction reaction is believed to pro-

ceed so rapidly (8) that it is responsible for forming the initial layer of tungsten, which interfaces with the silicon substrate. However, Levy *et al.* (2) recently demonstrated that no tungsten growth on silicon would occur if a sufficiently large amount of silicon tetrafluoride was present in the deposition ambient of hydrogen and tungsten hexafluoride. Since silicon reduction is suppressed by the presence of silicon tetrafluoride, it follows that hydrogen reduction cannot proceed on silicon in the absence of an already existing tungsten surface. In thermal LPCVD, this tungsten has to be supplied by silicon reduction. Therefore, the dominance of silicon reduction over hydrogen reduction in the initial phase of thermal LPCVD of tungsten may be more than a matter of faster reaction rate.

If the silicon surface participates actively in the silicon reduction reaction, it should be expected that the reaction itself be influenced by the method of surface preparation. Under certain deposition conditions, and for properly prepared silicon surfaces, silicon reduction is known to result in self-limiting tungsten deposition (8-12). Recently, Busta *et al.* (13) investigated the effects of native silicon oxide thickness on silicon reduction and observed a direct proportionality between the amount of oxygen at the tungsten/silicon interface and the amount of the native oxide.

In the present study, we have investigated the effects of two different cleaning procedures (14) on the silicon reduction of tungsten hexafluoride. One procedure ends

*Electrochemical Society Student Member.

**Electrochemical Society Active Member.

¹On leave from Central Research Laboratory, Hitachi Limited, Kokubunji, Tokyo, Japan.

²Present address: Department of Material Science and Engineering, Stanford University, Stanford, California 94305.

with a final HF cleaning, while the other does not. If it is assumed that the principal effect of the HF treatment is to remove the chemical oxide grown during the cleaning before the HF treatment, then a layer of chemical oxide would have been left on the samples without the HF treatment.

Experimental

Phosphorus doped 5-10 Ω -cm, (100)-oriented, 3 in. silicon wafers were used. The wafers were cleaned in freshly prepared solutions as follows: 10 min in 3:1 mixture of H_2SO_4/H_2O_2 at 90°C, 4 min of deionized (DI) water rinse; 10 min in 1:1:5 mixture of $HCl/H_2O_2(30\%)/H_2O$ at 70°C, 4 min DI water rinse; 10 min in 1:1:5 mixture of $NH_4OH(30\%)/H_2O_2(30\%)/H_2O$ at 70°C, 4 min of DI water rinse. The wafers were split at this point with half of them receiving a 30s dip in 50:1 H_2O/HF . All wafers were immediately loaded into the reactor after a final DI water rinse and heated nitrogen spin dry.

Tungsten deposition was done in a tubular hot wall low pressure reactor (15) at a pressure of 300 mtorr, and a temperature of 305°C. The wafers were placed with the surfaces perpendicular to the direction of the gas flow. After the wafers were loaded, roughly 1h was allowed for the reactor to reach stable deposition conditions. The ambient during the stabilization period was high purity nitrogen at a flow rate of 500 cm^3 . Tungsten hexafluoride at 10 cm^3 was then injected to initiate the reaction. Five different deposition times were chosen: 3, 6, 12, 24, and 36 min.

Results

The thickness of the chemical oxide on the samples without the HF treatment was measured directly using cross-sectional TEM and found to be about 17Å. The native oxide thickness on the samples with the HF treatment, estimated using an ellipsometer, was consistently less than 5Å.

Electrical.—Sheet resistance maps were generated using a Prometrix four-point probe setup. The average sheet resistance in the center regions of the wafers is plotted as a function of the deposition time in Fig. 1.

For samples with the HF treatment (without the chemical oxide), the sheet resistance values showed no systematic change for the various run times. The sheet resistance was consistently lower at the centers of the wafers and increased towards the edges. This might be caused by the nonuniformity in the gas-phase distribution of reactants and products. Sheet resistance uniformity improved with longer run time, with the standard deviation dropping from 23% for the 3 min run to 12% for the 36 min run. The thickness of the tungsten films was estimated using Auger depth profiling, and a thickness of about 110Å was consistently obtained for all of the samples. Using an average measured sheet resistance of 20 Ω/\square , one can estimate the resistivity to be 30 $\mu\Omega$ -cm.

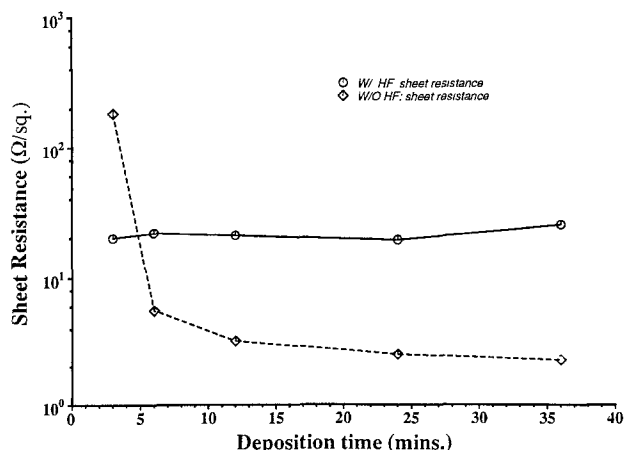


Fig. 1. Sheet resistance of samples with and without the HF treatment vs. deposition time.

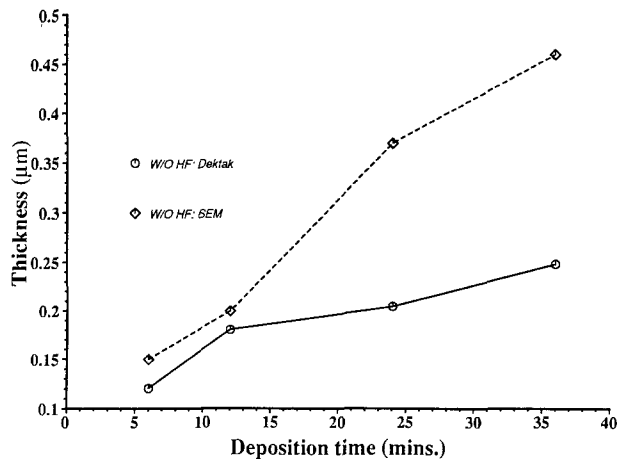


Fig. 2. Tungsten thickness of samples without the HF treatment vs. deposition time.

All of these results agree with the self-limiting reaction mechanism (8, 10, 11).

For samples without the HF treatment (with the chemical oxide), the sheet resistance dropped quite abruptly from the 3 min run to the 6 min run, and decreased gradually thereafter. The sheet resistance for the 3 min run was almost the same as that of the original silicon substrate, indicating the absence of a continuous tungsten film. SEM observation confirmed that selective nucleation had occurred without continuous film formation. Further deposition caused the growth and coalescence of the nucleated tungsten, resulting in an abrupt drop in sheet resistance. Deposition continued even after the nuclei coalesced and sheet resistance as low as 2.65 Ω/\square was measured for the 36 min run. Though there was still the tendency for the sheet resistance to increase towards the edges of the wafers, the uniformity was better than that for the samples with the HF treatment. The largest standard deviation was 12% for the 24 min run.

Tungsten thickness (Fig. 2) was estimated using a Dektak surface profilometer. Very thick films were obtained, starting with 1200Å for the 6 min run and increasing to 2500Å for the 36 min run. It is clear that self-limiting growth did not occur in these samples.

Our work agrees with previous observations (13) that the presence of a thin layer of silicon oxide would result in thick film deposition via silicon reduction. The reason for the unlimited growth has not been explained previously and will be the subject matter of this paper.

Auger electron spectroscopy (AES).—AES sputter profiling using a Xe ion beam was done in a Varian system (14). A square area of about 0.25 mm^2 was probed and a 400Å thick tungsten film standard was used to determine the sputtering rate.

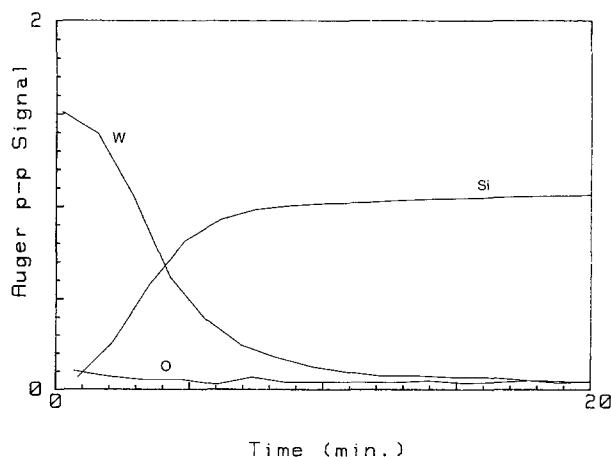


Fig. 3. Auger sputtering profile of samples with the HF treatment

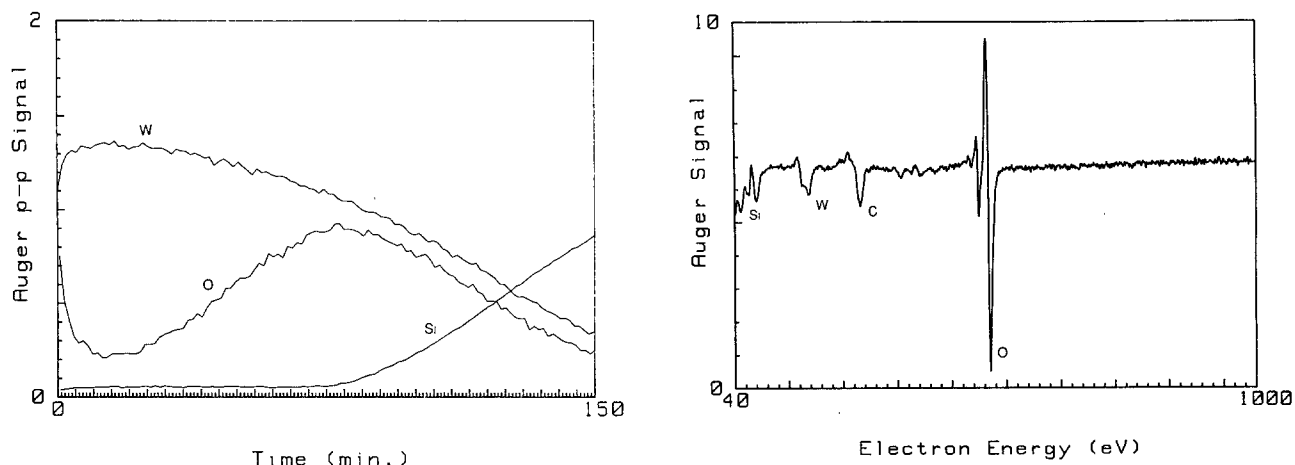


Fig. 4. (a, left) Auger sputtering profile of samples without the HF treatment. (b, right) Surface Auger spectrum of samples without the HF treatment.

For samples with the HF treatment, the Auger depth profile for the 36 min sample (Fig. 3) shows a very thin (100Å) tungsten film, thus confirming self-limiting growth. The oxygen Auger signal is quite low in the film, indicating a low level of oxygen contamination derived from the deposition. On the other hand, the Auger spectrum of the surface before sputtering indicates a high level of oxygen contamination, probably caused by atmospheric contamination (e.g., oxygen, moisture, and carbon dioxide adsorption) on the surface when the sample was exposed to air. No detectable silicon Auger signal was observed on the surface.

The Auger depth profile (Fig. 4a) for the 12 min sample without the HF treatment shows thick tungsten deposition, in agreement with the surface profilometer measurement results. The oxygen Auger signal shows a surface peak, which again is probably caused by atmospheric contamination when the sample was exposed to air. Below the surface, the oxygen signal level drops and then rises before dropping again as the silicon signal level begins to rise. Integrating the oxygen signal for this sample indicates the presence of a large amount of oxygen in the film, almost equivalent to the oxygen content in 100Å of silicon dioxide. It is impossible to obtain such a thick layer of oxide with the prescribed cleaning procedure. Unlike the case for samples with the HF treatment, Auger spectra for samples without the HF treatment indicated the presence of silicon (Fig. 4b) on the surface.

This silicon signal disappeared after 1 min of sputtering.

The origin of the large amount of oxygen in the film and of the silicon on the surface will be discussed in the Discussion section.

Scanning electron microscopy (SEM).—SEM observations of the samples without the HF treatment will be described.

The plan-view micrograph (Fig. 5a) of the 3 min sample clearly shows tungsten nuclei distributed over the surface. The nuclei show a range in size from the limit of the SEM resolution (20-30Å) to an upper diameter of several thousand angstroms. The larger nuclei appeared to have a granular texture, some with center voids surrounded by tungsten with a spiraling structure. Silicon was detected inside these voids by scanning AES (16). When the sample was observed at an oblique angle (Fig. 5b), these larger nuclei turned out to be depressions in the silicon surface with some granular edge features protruding above the substrate surface.

The 6, 12, 24, and 36 min samples will be considered as a group. All surfaces (Fig. 6a-d) are decorated with numerous spots with darker contrast, the densities and sizes of which change very little among the samples. From micrographs of higher magnification (Fig. 7a), the diameters of these spots can be estimated to be around 1000Å. A cross-sectional micrograph (Fig. 7b) shows that

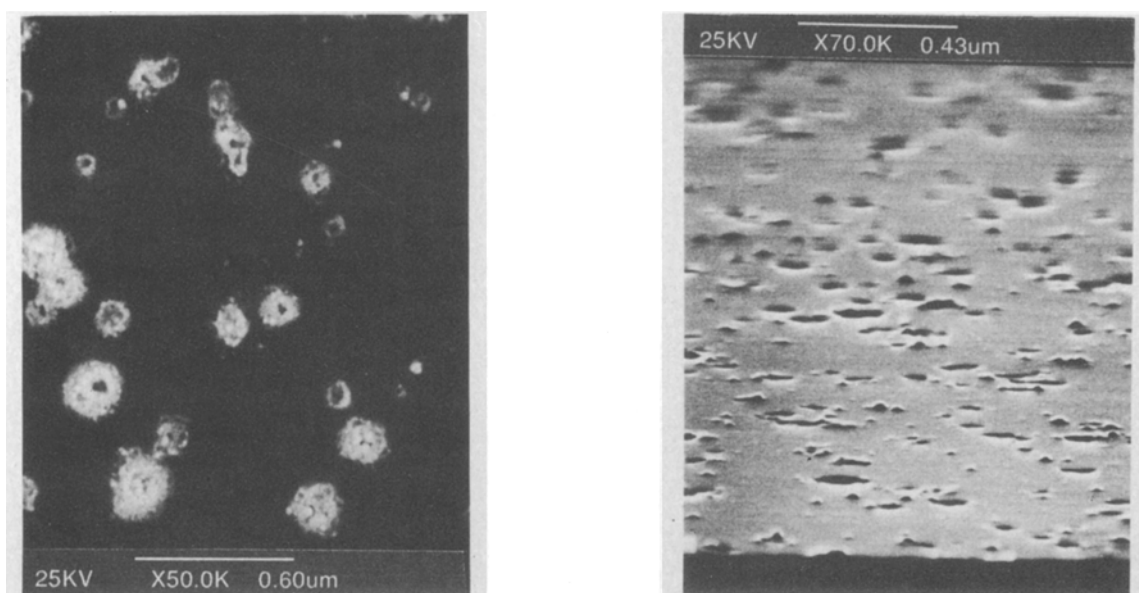


Fig. 5. (a, left) SEM micrograph of the 3 min sample showing disjointed nucleation. (b, right) SEM micrograph taken at an oblique angle. Disjointed nuclei correspond to depressions on the silicon surface.

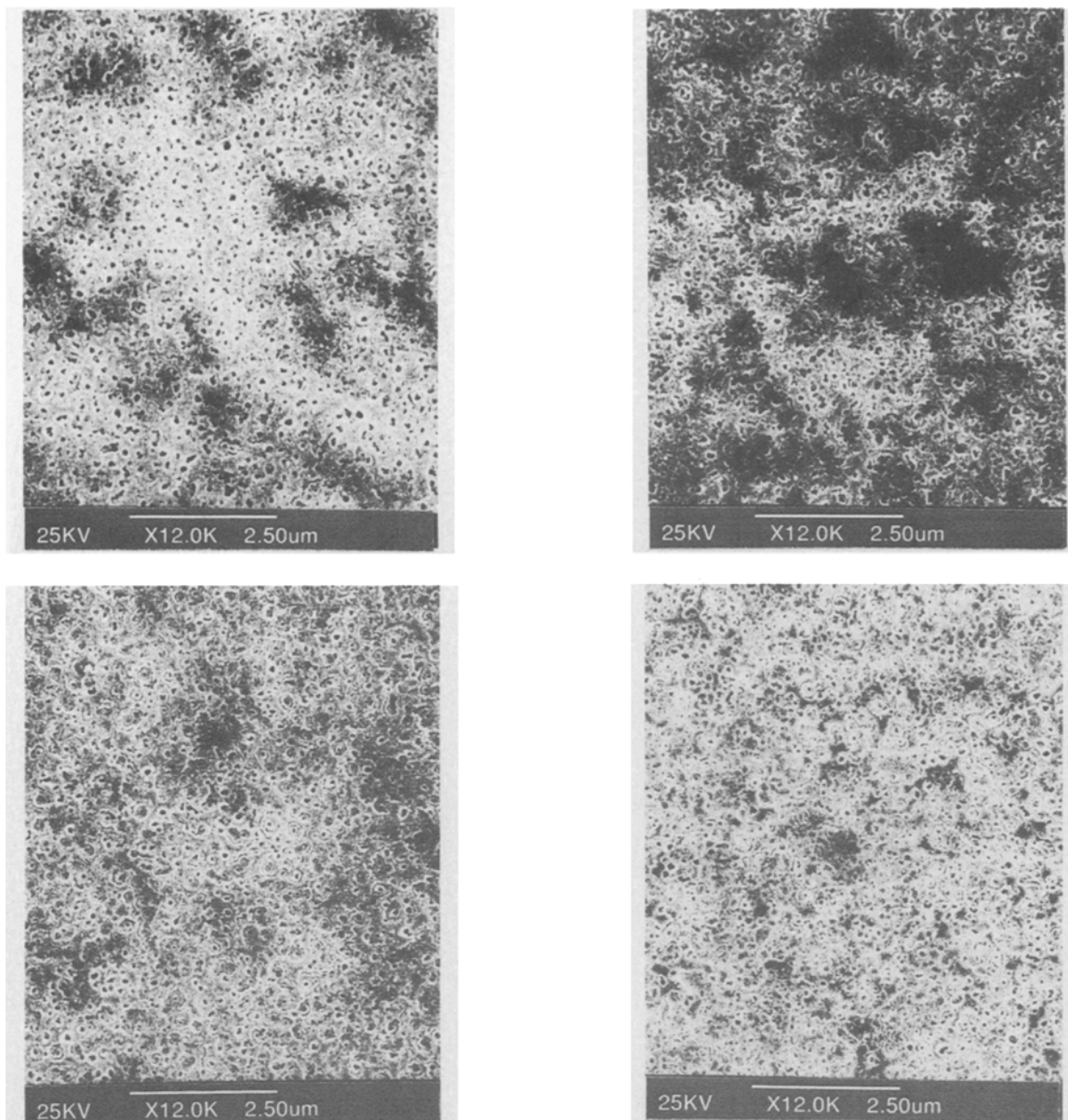


Fig. 6. (a, top left) Plan-view SEM micrograph of the 6 min sample. (b, top right) Plan-view SEM micrograph of the 12 min sample. (c, bottom left) Plan-view SEM micrograph of the 24 min sample. (d, bottom right) Plan-view SEM micrograph of the 36 min sample.

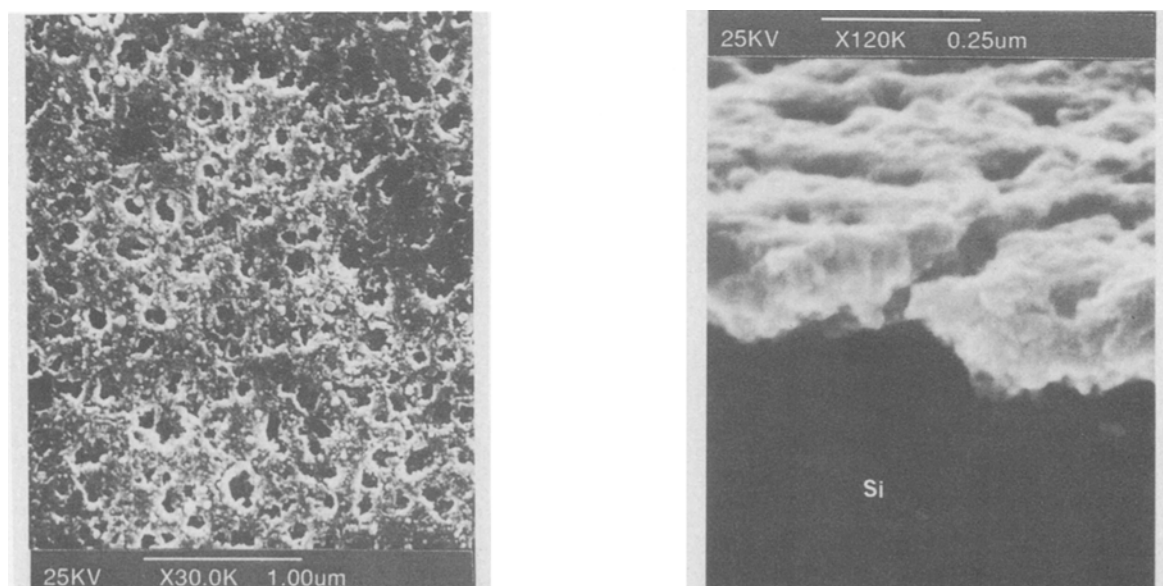


Fig. 7. (a, left) Plan-view SEM micrograph of the 12 min sample at a higher magnification showing size and density of the spots of darker contrast. (b, right) Cross-sectional SEM micrograph of a channel through the tungsten film.

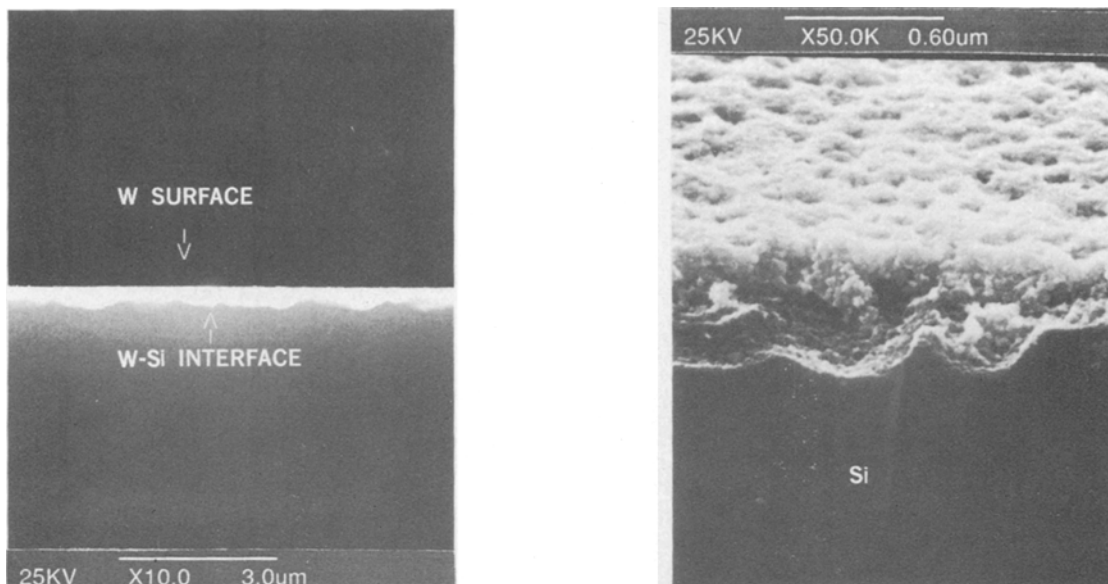


Fig. 8. (a, left) Roughness contrast between tungsten surface and tungsten/silicon interface. (b, right) Cross-sectional SEM micrograph of rough silicon surface with the tungsten partly removed.

such spots correspond to channels going from the surface, through the tungsten film, and terminating in the silicon substrate. It is also apparent from the cross-sectional micrograph (Fig. 8a) that the tungsten/silicon interface is much rougher than the tungsten surface. Figure 8b shows the rough silicon surface when the tungsten film was partly removed.

The thickness of the tungsten films (Fig. 2) was estimated using cross-sectional SEM and plotted along with that measured using the surface profilometer. The surface profilometer measurements were smaller because of the large radius (12.5 μm) of its probe tip and therefore not as accurate as those obtained using SEM.

Transmission electron microscopy (TEM).—As expected for a self-limiting film, the plan-view TEM micrograph (Fig. 9) of a sample with the HF treatment shows a continuous film of tungsten with no gross porosity like the voids observed in the tungsten films without the HF treatment.

For a sample without the HF treatment, a cross-sectional TEM micrograph (Fig. 10a) of a nucleation site shows a void in the silicon substrate half filled with tungsten. The recessed tungsten nucleus is aligned to one side of the void with a small overgrowth above the original silicon surface. The presence of this overgrowth is an indication that some chemical species must be mobile enough to migrate on top of the nucleus during the nucleation process. The cross-sectional TEM micrograph (Fig. 10b) of a more developed nucleation site shows the porous nature of the boundary between the tungsten nucleus and the silicon substrate. Tungsten hexafluoride can diffuse along this porous periphery and react with exposed silicon, causing the nucleus to grow.

Discussion

The silicon reduction reaction results in the removal of slightly less than two unit volumes of silicon for every unit volume of tungsten deposited (8). Depending on how this extra volume of void is displaced, the character of the deposition can be very different.

Since self-limiting deposition was obtained for samples with the HF treatment (without the chemical oxide), the volume of void must have been displaced mostly in the direction normal to the wafer surface (Fig. 11a). The silicon surface is sealed and the deposition is self-limiting.

The situation is more complicated for the samples without the HF treatment (with the chemical oxide). As indicated in the section on AES, the amount of oxygen in the tungsten film could not be totally ascribed to the chemical oxide. Besides, it would be surprising to ob-

serve tungsten nucleation and growth on silicon covered with such a thick oxide (13). In fact, no tungsten was observed on samples with 1000 \AA of thermally grown oxide, even after 36 min of exposure to tungsten hexafluoride under identical deposition conditions. This implies that the reaction between tungsten hexafluoride and silicon dioxide, though thermodynamically favorable (17), must be kinetically very slow at this deposition condition. We believe the initial selective tungsten nucleation started in "weak" spots (8, 18) of the chemical oxide, *e.g.*, physical weak spots such as pin holes or chemical weak spots such as silicon-rich silicon oxide. This reaction consumes silicon, deposits tungsten, and generates a void. In the presence of the chemical oxide, not all of the void volume is displaced away from the substrate surface. Lateral volume displacement leaves the tungsten film punctuated with channels (Fig. 11b). Such channels, penetrating all the way from the surface of the tungsten to the tungsten/silicon interface, allow tungsten hexafluoride to reach the silicon substrate and enable silicon reduction to proceed continuously along the tungsten/silicon interface.

TEM observations confirmed the lateral displacement of void volume (Fig. 10a) in the initial stage of tungsten nucleation. It would seem that the voids at the centers of the nucleation sites (Fig. 5a), which are surrounded by spiraling structures as observed by SEM and TEM, are to be associated with the channels in the thicker films.

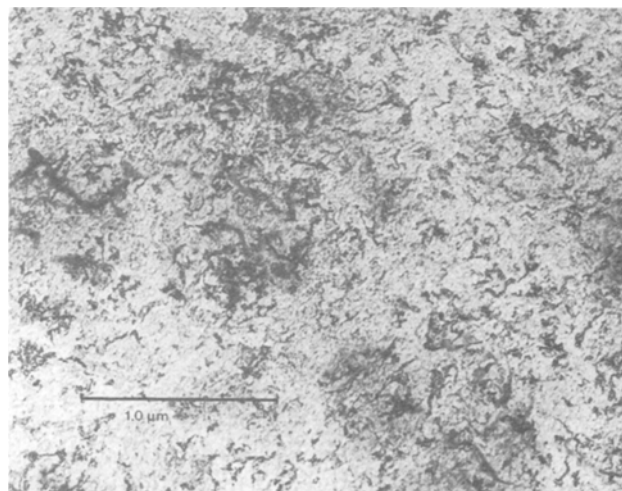


Fig. 9. Plan-view bright-field TEM micrograph of self-limiting film

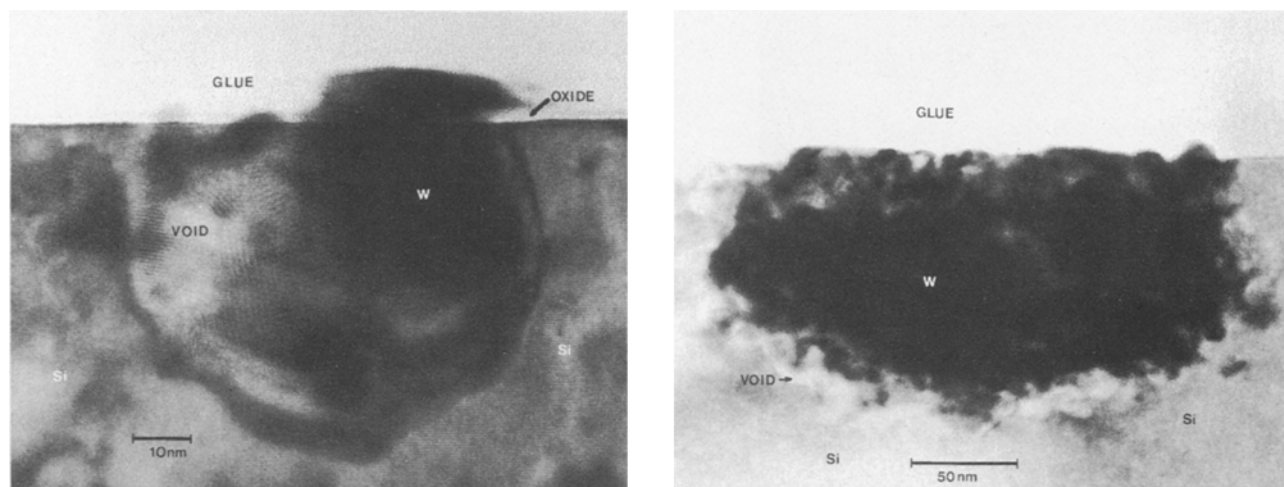


Fig. 10. (a, left) Cross-sectional TEM micrograph of a tungsten nucleus. (b, right) Cross-sectional TEM micrograph showing porous periphery

Many of these channels show similar spiraling effects (Fig. 7a). As the nuclei grew sideways, the chemical oxide would be weakened and new nucleation sites would be generated. The portions of the film resulting from these new sites would be thinner, thus explaining the roughness of the tungsten/silicon interface. Therefore, the apparent compositional gradient indicated by the tungsten Auger signal (Fig. 4a) is caused by the nonuniformity (Fig. 8a) in the tungsten thickness. Conversely, since the tungsten/silicon interface is the actual growth front, the tungsten surface remains more or less at the level of the original silicon surface and retains its smoothness.

The surface silicon Auger signal should be due to the original chemical oxide scattered on the surface. This chemical oxide will not be scattered throughout the film as long as the tungsten/silicon interface can be identified as the growth front. Since there was no chemical oxide on the samples with the HF treatment, surface silicon Auger signal was not detected in these samples.

The large amount of oxygen in the film can also be explained in terms of atmospheric contamination on the sidewalls of the channels, when the samples were exposed to air. The concurrent rising of the silicon Auger signal (Fig. 4a) with the peaking of the oxygen Auger signal is an indication of the depth below the tungsten surface where a large number of channels terminate. Silicon

at the end of these channels provides additional area for oxygen or moisture adsorption. Therefore, the amount of oxygen should be correlated with the surface area available for adsorption, rather than be correlated with the amount of silicon oxide originally present on the silicon surface (13). The higher resistivity (greater than $60 \mu\Omega\text{-cm}$) of the thick films should be explained in terms of the porous and granular nature of the film. Oxygen, mostly originated from atmospheric adsorption on exposed tungsten surfaces and hence not being incorporated in the film, is not expected to be a major factor in causing the higher resistivity.

If tungsten nucleation and growth require the presence of silicon, and silicon can only be found at the end of the channels, it is obvious why the densities and sizes of the dark spots observed in the plan-view SEM micrographs did not change with deposition time. The channels would not close if no tungsten growth could take place on the sidewalls.

Finally, the presence of tungsten overgrowth (Fig. 10a) above the silicon surface is an indication that some chemical species must be mobile. One possibility is that tungsten atoms, once formed on the silicon surface, migrated around until attaching to an existing tungsten nucleus. The atoms remained mobile on the surface of the tungsten nucleus before finally being captured in suitable incorporation sites and became part of the nucleus.

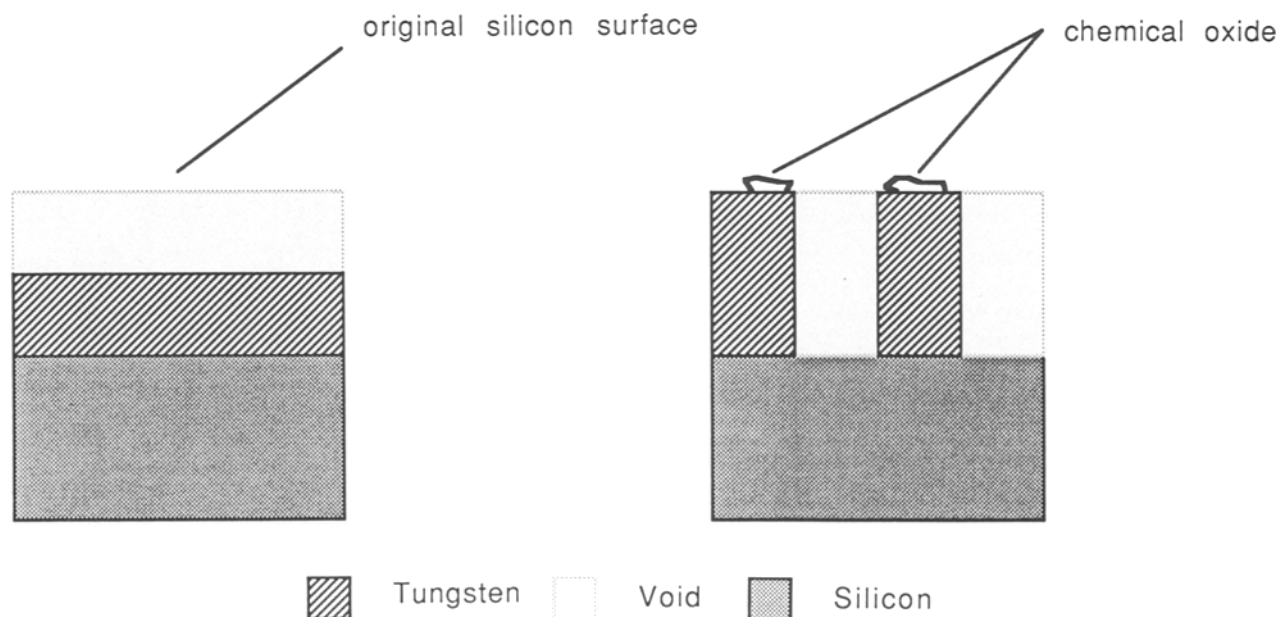


Fig. 11. (a, left) Vertical volume reduction. (b, right) Horizontal volume reduction

Summary

Thick tungsten deposition via the silicon reduction of tungsten hexafluoride was obtained when a layer of chemical oxide was deliberately left on the silicon surface. The thick films are punctured with microchannels penetrating all the way from the tungsten surface to the tungsten/silicon interface. We believe the chemical oxide causes horizontal volume reduction to occur, thus generating the microchannels. Tungsten hexafluoride can easily diffuse along these channels to reach the silicon substrate, causing unlimited tungsten growth.

Acknowledgment

This work was supported by the SRC under contract no. 83-01-006.

Manuscript submitted Jan. 12, 1987; revised manuscript received March 24, 1987.

Stanford University assisted in meeting the publication costs of this article.

REFERENCES

1. S. Swirhun, K. C. Saraswat, and R. M. Swanson, *Electron Device Lett.*, **EDL-5**, 209 (1984).
2. R. A. Levy, M. L. Green, P. K. Gallagher, and Y. S. Ali, *This Journal*, **133**, 1905 (1986).
3. J. G. Black, D. J. Ehrlich, J. H. C. Sedlacek, A. D. Feinerman, and H. H. Busta, *Electron Device Lett.*, **EDL-7**, 422 (1986).
4. R. H. Wilson, R. W. Stoll, and M. A. Calacone, in "1985 Proceedings IEEE VLSI Multilevel Interconnection Conference," p. 343, IEEE, New York (1985).
5. N. Kobayashi, N. Hara, S. Iwata, and N. Yamamoto, in "1986 Proceedings IEEE VLSI Multilevel Interconnection Conference," p. 436, IEEE New York (1986).
6. G. C. Smith, in "1985 Proceedings IEEE VLSI Multilevel Interconnection Conference," p. 350, IEEE New York (1985).
7. W. A. Bryant, *This Journal*, **125**, 1534 (1978).
8. E. K. Broadbent and C. L. Ramiller, *ibid.*, **131**, 1427 (1984).
9. W. T. Stacy, E. K. Broadbent, and M. H. Norcott, *ibid.*, **132**, 444 (1985).
10. H. Itoh, R. Nakata, and T. Moriya, *IEEE IEDM*, 606 (1985).
11. K. Y. Tsao and H. H. Busta, *This Journal*, **131**, 2707, (1984).
12. D. C. Paine, J. C. Brayman, and K. C. Saraswat, in "Proceedings 1985 Workshop on Tungsten and Other Refractory Metals for VLSI Applications," p. 117, Materials Research Society, Pittsburgh, PA (1985).
13. H. H. Busta and C. H. Tang, *This Journal*, **133**, 1195 (1986).
14. N. Kobayashi, M. Wong, R. Browning, K. C. Saraswat, and C. R. Helms, Submitted to *Appl. Phys. Lett.*
15. K. C. Saraswat, S. Swirhun, and J. P. McVittie, in "VLSI Science and Technology/1984," K. E. Bean and G. A. Rozgonyi, Editors, p. 409, The Electrochemical Society Softbound Proceedings Series, Pennington, NJ (1984).
16. R. Browning, *J. Vac. Sci. Technol. A*, 1453 (1984).
17. J. Carlsson and M. Boman, *J. Vac. Sci. Technol.*, **3**, 2298 (1985).
18. A. G. Revesz and H. A. Schaeffer, *This Journal*, **129**, 357 (1982).

Impurity Doping during Si Epitaxy by Means of CO₂ Laser CVD

T. Meguro,¹ O. Okabayashi, and T. Itoh*

School of Science and Engineering, Waseda University, Ohkubo, Shinjuku-ku, Tokyo 160, Japan

ABSTRACT

Impurity doping during the Si epitaxial growth by means of CO₂ laser CVD is reported. We have grown n-type single crystalline Si on (100) Si substrate using SiH₄ as a Si source and PH₃ as a donor impurity at growth temperatures T_s between 550° and 750°C. The electron mobilities at room temperature of Si films grown at 600°C were near values of bulk crystal for the corresponding carrier concentrations, while the electron mobilities of Si films grown at 700°C were about 10% of the bulk values. From the transmission electron microscope (TEM) observation, it was clarified that the degradation of the electron mobility at 700°C was caused by the segregation of P atoms in the Si epilayer.

Several researchers (1-7) have investigated thin film formation by means of CO₂ laser CVD method. Bilenchi *et al.* (6) have reported on the successful growth of doped a-Si:H films. In our previous report (7), the low temperature undoped Si epitaxial growth using SiH₄ by CO₂ laser CVD was described. There is a strong advantage in decreasing T_s to prevent impurity redistribution by indiffusion across the interface. In the case of conventional low temperature Si epitaxy by CVD, however, there was a tendency of poor dopant activation, generally caused by the dopant atoms which were placed off the preferable surface sites due to the volume reaction. It is advantageous to promote the surface reaction and to eliminate the volume reaction for the epitaxial growth by CVD. Since the decomposition of source gas proceeds on the surface in the case of CO₂ laser CVD (7), it is expected that doped Si epitaxial growth will occur at low temperature.

In this paper we discuss low temperature Si epitaxy of P doped n-type single crystalline Si by means of the CO₂ laser CVD using SiH₄ containing PH₃.

*Electrochemical Society Active Member.

¹Present address: The Institute of Physical and Chemical Research (RIKEN), Wako-shi, Saitama 351-01, Japan.

Experiment

The CO₂ laser epitaxy system used in this study was described in detail in the previous report (7). A p-polarized 50W cw CO₂ laser beam 25 mm in diam was directed on the Si substrate at a 45° angle of incidence and the wavelength of CO₂ laser was fixed at 10P(20) in the present work.

Substrates were n-type (100) oriented single crystalline Si wafers with the resistivity above 100 Ω-cm for Hall measurements. The partial pressure of 100% PH₃ contained in the SiH₄ was varied between 1×10^{-6} and 1×10^{-4} torr, corresponding to a pressure ratio of PH₃/SiH₄ from 20 to 2000 ppm. Substrates were heated by a resistive heated carbon plate and Si films were grown at T_s between 550° and 750°C. The single crystalline films grown at 650°C had a growth rate of 1.5 nm/s using 0.05 torr of 100% SiH₄ pressure.

The carrier concentration and the electron mobility of films were obtained by the Hall measurement with van der Pauw method at room temperature. The growth rate was measured optically on angle lapped samples after staining 30s in HNO₃ containing a slight amount of HF. The crystalline quality and the surface morphology were observed by means of reflection high energy electron dif-